LANGMUIR Article
Cite This: Langmuir 2019, 35, 2814−2820
pubs.acs.org/Langmuir

Interfacial Behavior of Fumonisin B1 Toxin and Its Degradation on the Membrane

Shiv K. Sharma,[†] Sijan Poudel Sharma,[‡] Darlene Miller,[§] Jean-Marie A. Parel,[§] and Roger M. Leblanc*[,†]

[†]Department of Chemistry, University of Miami, 1301 Memorial Drive, Coral Gables, Florida 33146, United States
[‡]Department of Biology, University of Miami, 1301 Memorial Drive, Coral Gables, Florida 33146, United States
[§]Bascom Palmer Eye Institute, Miller School of Medicine, 900 NW 17th St., Miami, Florida 33136, United States

Supporting Information

ABSTRACT: Fumonisin B1 (FB1), the most abundant component of the fumonisin family, is highly responsible for fungal infections. In this paper, our main aim is to study the surface chemistry and spectroscopic properties of the FB1 molecule and observe the impact of green LED light on the FB1 Langmuir monolayer. From the surface chemistry and spectroscopic studies, we found that the FB1 molecule forms a self-assembled Langmuir monolayer which is sufficient to mimic its interaction with the corneal tissues. The irradiation of green LED light on the FB1 Langmuir monolayer showed the degradation of the FB1 when compared to that in the absence of light. This observation reveals that FB1 molecules lose their tendency to stay as a Langmuir monolayer. The degradation observed on the interface was compared with the bulk phase of FB1. The bulk phase observation also indicated the degradation tendency which reinforced the observed interfacial property of FB1.

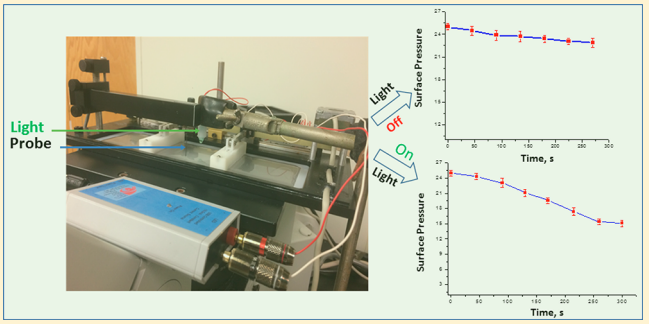

1. INTRODUCTION

Fungal infections are mainly caused by filamentous or yeast-like fungi.[1,2] Among different filamentous fungi, the *Fusarium* species are most widely linked with corneal infections.[3] Fumonisins are a group of mycotoxins produced by the *Fusarium* species.[4] These are taxonomically challenging mycotoxins which consist of linear carbon backbones substituted at various positions with hydroxyl, methyl, and tricarboxylic acid groups.[5] Apart from corneal infections, these fumonisins are also responsible for esophageal cancer.[6] The International Agency for Research on Cancer (IARC) has assessed the cancer probability of fumonisins to humans and classified them as group 2B.[7] Fumonisins are usually extracted in aqueous methanol or aqueous acetonitrile.[8,9] Among the different fumonisins, we are interested in Fumonisin B1 (FB1), as this molecule is the most prevalent of the fumonisins in naturally contaminated corn and is usually present as 70% of the total fumonisins detected.[10]

Historically, there has been an intensive challenge in the proper treatment of fungal infections of the cornea due to the sensitivity of the visionary organ. Several methods like keratoplasty,[11] corneal cross-linking,[12] and antifungal medication[13,14] have experienced different set-backs.[3,15] In this perspective, the light treatment method has been regarded as the safest method in the treatment of fungal infections.[16,17] In our previous study, we first treated the cornea with Rose Bengal, a photosensitizer, and later, green light was applied to degrade the actual fungus. We found that green light alone has no effect on the fungus.[18,19] In the due course of study, apart from fungus, we were interested to know the interfacial property of FB1 and the effect of green LED light alone on its Langmuir monolayer. Our interfacial work showed that the FB1 Langmuir monolayer gets degraded with the application of green LED light.

The FB1 Langmuir monolayer degradation is directly related to the change in interaction of the toxin with the corneal tissue. The study of the interactions between invading fungi and host cells is important in the study of fungal infections of the cornea.[20] The interaction occurs due to the adherence property of the toxin. Fungal pathogens have a variety of adhesins that can interact with native cell proteins and glycoproteins.[21] Surface chemistry study is a powerful tool to mimic the interaction of the analyte with the cell membrane.[22] Further, the surface chemistry study approach via the Langmuir monolayer technique facilitates the study of cell adhesion and its implications. This is very important as most mammalian cells are adherent. Therefore, the surface chemistry

Received: October 18, 2018
Revised: December 13, 2018
Published: January 23, 2019

DOI: 10.1021/acs.langmuir.8b03505
Langmuir 2019, 35, 2814−2820

study of FB1 will provide sufficient information about the interaction of this toxin with the host cell.

In this paper, we first studied the surface chemistry and spectroscopic properties of the FB1 Langmuir monolayer to mimic the process of interaction of the toxin with the cell membrane. Later, we treated the FB1 Langmuir monolayer with green LED light. We were aware of the fact that LEDs do not produce energy at a single wavelength (as lasers do). The green LED we selected emits light over a certain bandwidth; the 525 nm LED emission curve shows the LED 20% energy values being between 500 and 550 nm.

To the best of our knowledge, the interfacial property of FB1 toxin has not been studied until now although it is of utmost important to know the interaction of the toxin with the cell membrane. Further, the impact of light on the FB1 Langmuir monolayer remains unknown. We designed a new methodology to observe the degradation of FB1 on the membrane. We hope that this investigation will open new avenues in the treatment of fungal infections.

2. EXPERIMENTAL SECTION

2.1. Materials and Reagents. Fumonisin B_1 extracted from *Fusarium moniliforme* > 98% (HPLC) was obtained from Sigma-Aldrich, Co., St. Louis, MO, United States. The water that was utilized in the experiments was obtained from PURELAB Ultra, Elga Lab Water (Veola Water Solutions and Technologies, U.K.) with a resistivity of 18 MΩ cm, a surface tension of 71.6 mN·m^{-1}, and a pH of 7.4. Methanol required to dissolve FB1 was received from M.P. Biomedicals LLC, Santa Ana, CA, United States.

2.2. Equipment. All experiments were carried out in a Clean Room (class 1000) in which the temperature (20.0 ± 0.5 °C) and humidity (50% ± 1%) were maintained constantly. In the study of surface pressure−area (π−A) isotherms, and compression/decompression cycles, a Kibron μ-trough (Kibron Inc., Helsinki, Finland) having an area of 124.5 cm^2 (5.9 cm × 21.1 cm) was used. The Wilhelmy method was employed to assess the surface pressure with a 0.51 mm diameter alloy wire probe with a sensitivity of ±0.01 mN·m^{-1}. For the in situ UV−vis experiment, we used a KSV mini-trough (KSV Instrument Ltd., Helsinki, Finland) with an area of 225 cm^2 (7.5 × 30 cm).

2.3. Methods. *2.3.1. Surface Pressure−Area Isotherm Preparation.* FB1 dissolved in aqueous methanol was diluted with pure water to achieve a concentration of 2.8 × 10^{-4} M (0.2 mg.mL^{-1}) and pH 7.4. The pH of 7.4 was chosen to equilibrize the pH of human corneal stroma.[23] The FB1 was uniformly spread over the air−water interface by the use of a 100 μL syringe (Hamilton Co., Reno, Nevada). The spreading volume of the toxin solution was 45 μL for the surface chemistry and spectroscopic measurements. After the solution was spread, the Langmuir monolayer reached equilibrium after 12−15 min. Then, the Langmuir monolayer was compressed at a rate of 12 Å^2·molecule^{-1}·min^{-1} such that the compression process was complete in around 10 min to maintain consistency in the experiments. The experiments were repeated three times, and good reproducibility was achieved. The reason behind employing the Kibron μ-trough for the surface pressure and compression/decompression experiments and the KSV trough for the in situ UV−vis experiments is that the KSV trough provides plenty of space to continually relocate the UV−vis machine parts as compared to the Kibron trough.

2.3.2. UV−vis Absorption Spectroscopy. The UV−vis absorption spectra of the FB1 Langmuir monolayer at the air−water interface was measured by a UV−vis diode array spectrophotometer (Hewlett-Packard, model 8452A, Palo Alto, CA) on the top of a KSV mini Langmuir trough (KSV Instruments Ltd., Finland). A quartz window is fitted in the middle of the trough to facilitate the passing of the beam through the Langmuir monolayer and the water subphase. The spectra were obtained initially at 0 and 1 mN m^{-1}, and at every 5 mN m^{-1}, surface pressures increment onward under dark environment up to 20 mN m^{-1}.

2.3.3. Fluorescence Spectroscopy. The in situ fluorescence spectra of the FB1 Langmuir monolayer was measured with the help of an optical fiber detector stationed on the top of the KSV trough. The optical fiber was coupled to the Spex Fluorolog fluorespectrometer (Horiba, Jovin Yvon, Edison, NJ). The optical fiber used in the experiment had an area of 0.25 cm^2 and rested approximately 1 mm above the air−water interface. Initially, the excitation light gets transmitted through the optical fiber from the light source to the Langmuir monolayer and at the same time, the emitted light from the monolayer gets dispatched back to the detector through the optical fiber. This is how the data gets collected.

2.3.4. Compression/Decompression Cycles. To study the hysteresis of the film formed, the Langmuir monolayer of FB1 was first compressed from 0 to 15 or 23 mN m^{-1} and decompressed subsequently to 0 mN/m with a speed of 12 Å^2.molecule^{-1}.min^{-1}. This compression/decompression cycle was then repeated three times to reproduce the data.

2.3.5. Solution Work. Ultraviolet−visible spectroscopic measurements were obtained on an Agilent Cary 100 spectrophotometer (Santa Clara, CA, USA). The fluorescence spectra of the FB1 solution with and without treatment of light was measured with the help of the Spex Fluorolog Fluorespectrometer (Horiba, Jovin Yvon, Edison, NJ) having a slit width of 5 nm for excitation and emission. The mass spectra were obtained from a Bruker BioFlex IV Maldi-TOF mass spectrometer.

3. RESULTS AND DISCUSSION

3.1. Surface Chemistry Study. *3.1.1. Surface Pressure vs Area Isotherm.* Fumonisin B1 when spread on the water subphase shows that it has the capability to form a stable Langmuir monolayer. Figure 1 exhibits the surface pressure (π) versus mean molecular area (A) and the surface potential isotherms for the monolayer. It is a well-known fact that the air−water interface possesses excess free energy emanating from the difference in the environment between the surface molecules and those in the bulk. The spontaneous formation of the Langmuir monolayer when FB1 is placed on a liquid surface affects the surface tension. This surface tension can be viewed as a negative pressure due to the attractive interactions of the water molecules at the interface, which will be lowered by accumulation of the fumonisins at the air−water interface. The presence of a monomolecular film on a liquid surface

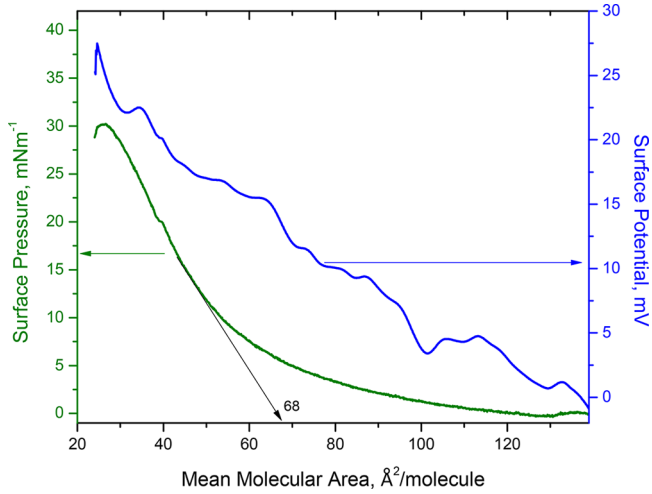

Figure 1. Surface pressure (π−A) and surface potential curve of Fumonisin B1.

DOI: 10.1021/acs.langmuir.8b03505
Langmuir 2019, 35, 2814−2820

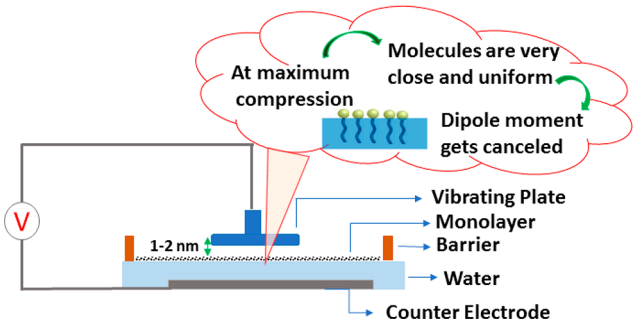

Figure 2. Capacitance method to measure surface potential by using vibrating plate.

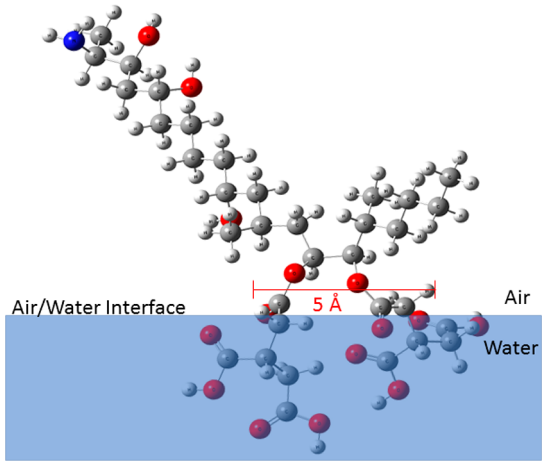

Figure 3. Simulation of FB1 molecule at the air–water interface to calculate its size.

invariably results in a reduction of the free energy of the system due to the creation of interactions between the hydrophilic polar group and the water surface molecules, thus reducing the surface tension. The resulting effect of the reduction of the surface tension leads to an expansion at the air–water interface in the presence of surfactants. The π–A isotherm measurement is the initial step to investigate the new materials spread on the subphase which provides insight into the existence of different phase transitions, packing, and the stability of a Langmuir monolayer, which ultimately acts as a model for studies of the interaction of the toxin, FB1, with the cell membrane of the cornea.

A surface potential measurement was carried out simultaneously with the surface pressure measurement to know the dipole moment or potential of the Langmuir monolayer above and beneath the monolayer by the use of a vibrating plate as shown in the schematic in Figure 2. In Figure 1, there is an immediate increase in surface potential in the gaseous phase, which is due to the change in dipole moment due to compression, stipulating that surface dipole forces and the orientation of the water (subphase) molecules result in a net interfacial orientation. The small bumps seen in the surface potential isotherm are due to the movement of FB1 molecules to gain a specific orientation on the subphase surface under the vibrating electrode. After the condensed phase was attained, we observed a decrease in the surface potential. This was due to the cancellation of the dipole–dipole moment due to the short distance.

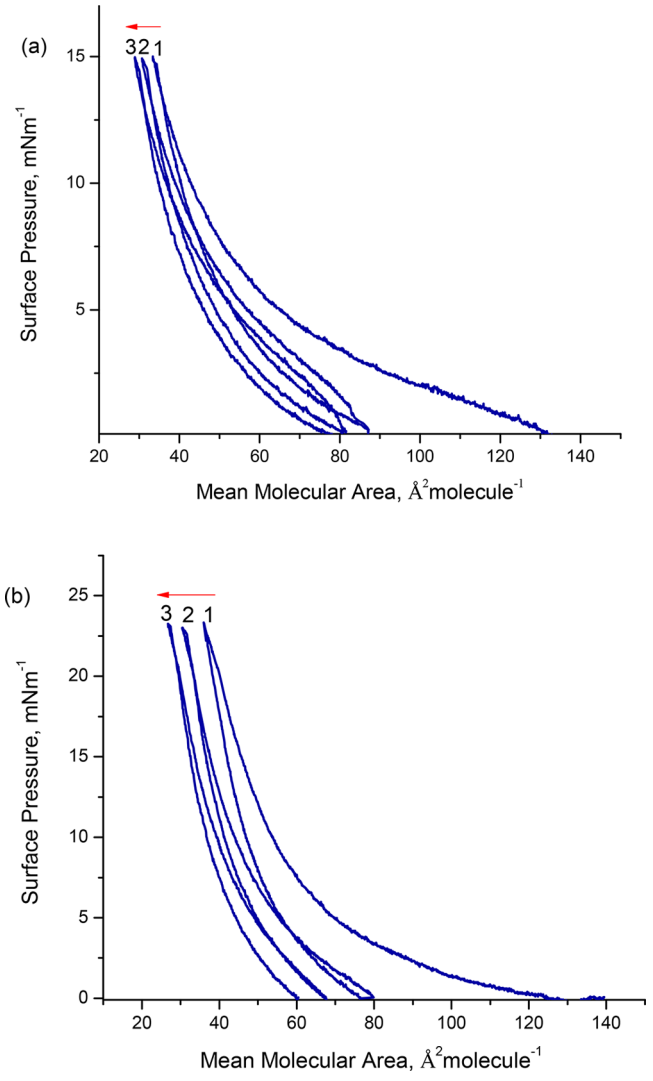

Figure 4. Compression/decompression π–A curves at two different surface pressures (a, 15 and b, 23 mN·m^{-1}).

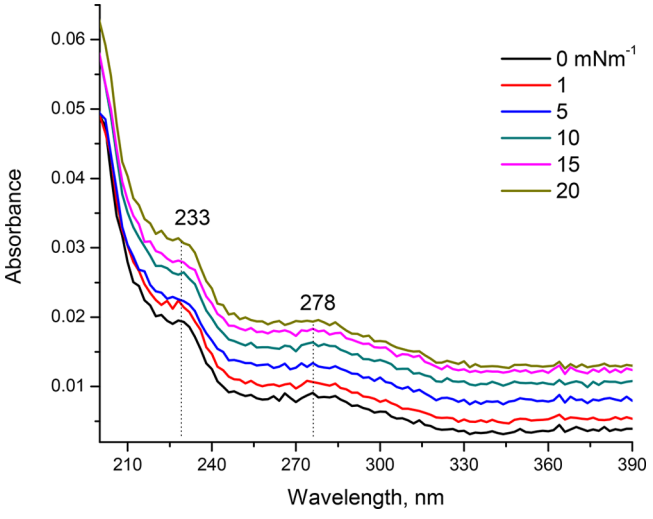

Figure 5. In situ UV–vis spectra of the FB1 Langmuir monolayer at different surface pressures.

In the π–A isotherm, the limiting molecular area of the FB1 Langmuir monolayer is 68 Å^2/molecule, as shown in Figure 1,

DOI: 10.1021/acs.langmuir.8b03505
Langmuir 2019, 35, 2814–2820

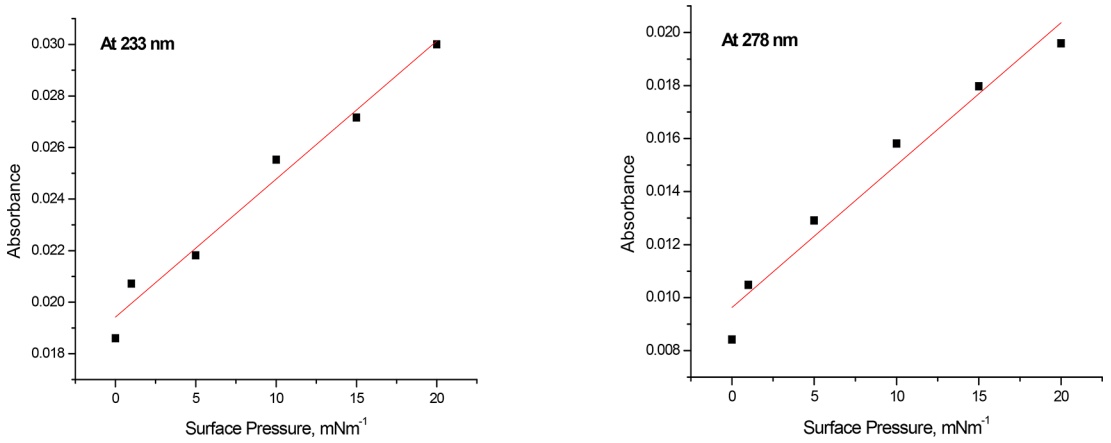

Figure 6. Plot of absorbance vs surface pressure at two different wavelengths: 233 and 278 nm.

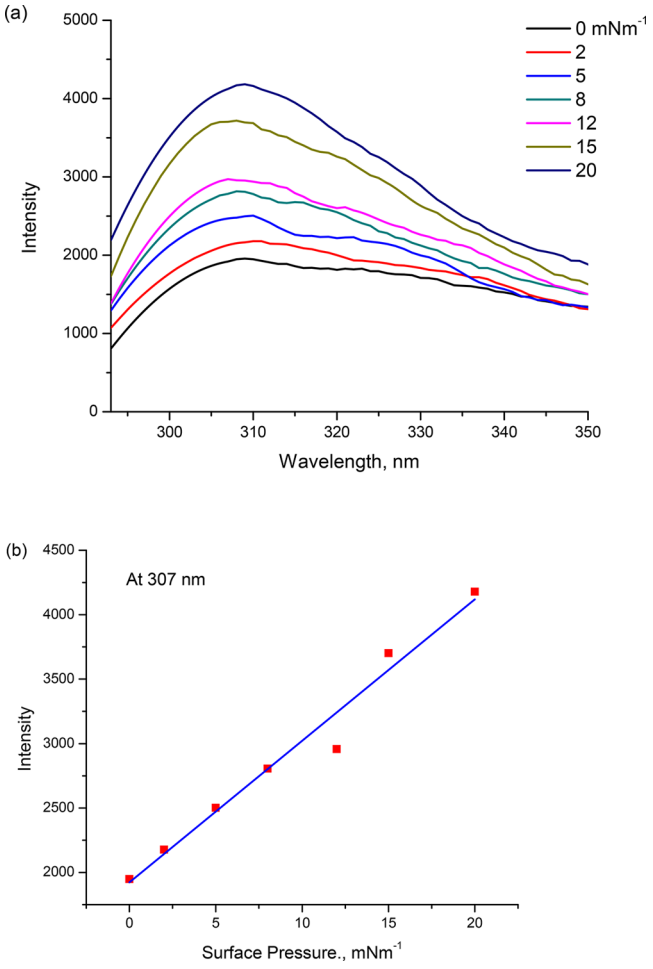

Figure 7. (a) In situ fluorescence spectra for the FB1 Langmuir monolayer at different surface pressures (b) and plot of intensity vs surface pressures at 307 nm.

that describes the minimum cross-sectional area per molecule. This value corresponds to the size of the FB1 molecule at the air−water interface to be 4.6 Å which is pretty close to the theoretical value of 5 Å, as shown in Figure 3, obtained by a computer program for modeling, simulation, and docking: YASARA.[24]

3.1.2. Compression/Decompression of the FB1 Langmuir Monolayer. The examination of the resistance of the FB1 Langmuir monolayer to external mechanical force at the air−water interface was performed by using compression/decompression cycles. Figure 4 shows the three compression/decompression cycles of the FB1 Langmuir monolayer at the air−water interface at two different surface pressures, namely, 15 and 23 mN·m^{-1}.

As FB1 is the most polar molecule in comparison to other fumoinsins,[25] our hypothesis was that some sort of hysteresis phenomena could be noticed for the FB1 Langmuir monolayer as opposite charges of polar molecules attract and charges that are alike repel. Per our hypothesis, for the successive three compression/decompression cycles that followed, it was found that a hysteresis behavior of the isotherm was witnessed. These cycles divulge that when compressed to 15 mN·m^{-1}, there is a small hysteresis due to the fact that a compact monolayer has not been formed yet. It has been found that only 8.0% of the initial isotherm has been reduced in comparison to the first and last cycle, whereas 23 mN·m^{-1} only exhibits a hysteresis difference of 11.0%. These results show that the FB1 molecules are reorganized at the interface while the water subphase contributes to this process. Beside the solubility of FB1 in the subphase, other possible explanations might be the alteration in the orientation and conformation of the toxin with time. This observation of the compression/decompression fortifies the explanation that the FB1, a toxin molecule, remains somehow active on the Langmuir monolayer which underpins the interaction in the toxin and cell membrane model.

3.1.3. In Situ UV−vis Absorption Spectroscopy of the Langmuir Monolayer. From the compression/decompression data, we found that the isotherm at higher surface pressure favors the hysteresis behavior. This hysteresis could be minimized and the stability could be increased by the addition of an electrolyte into the subphase.[26,27] But we wanted to create similar in vivo conditions as of the cell membrane to fit our model. So, we decided to perform in situ UV−vis absorption experiments without adding extra electrolyte. The absorption spectra at different surface pressures were recorded for the FB1 Langmuir monolayer as shown in Figure 5. Two different bands at 233 and 278 nm were observed. The maximum band at 233 nm corresponds to the $n-\pi^*$ transitions of the carboxylic groups which are abundantly present in the FB1 molecule. The band peak at 278 nm could possibly be due to the formation of intermolecular hydrogen bonding among the oxygen molecules of FB1 and hydrogen molecules of the water subphase.[28] With the compression of the monolayer to

DOI: 10.1021/acs.langmuir.8b03505
Langmuir 2019, 35, 2814−2820

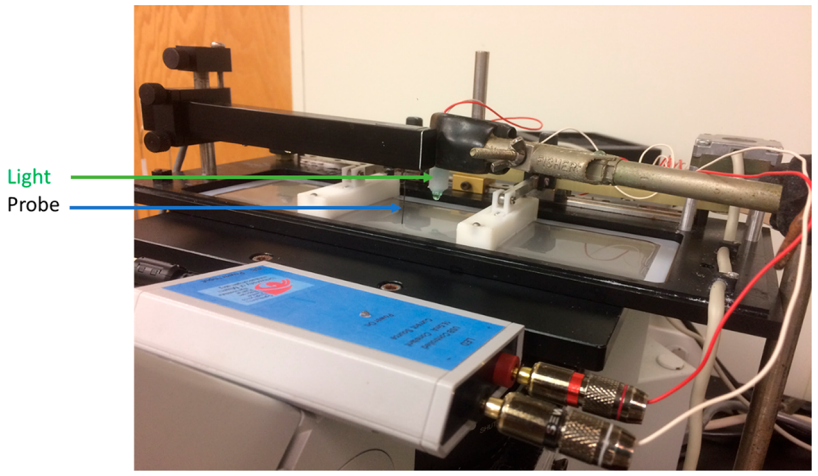

Figure 8. Kibron trough experimental setup with the adjusted green light source to study the effect of light on the FB1 Langmuir monolayer.

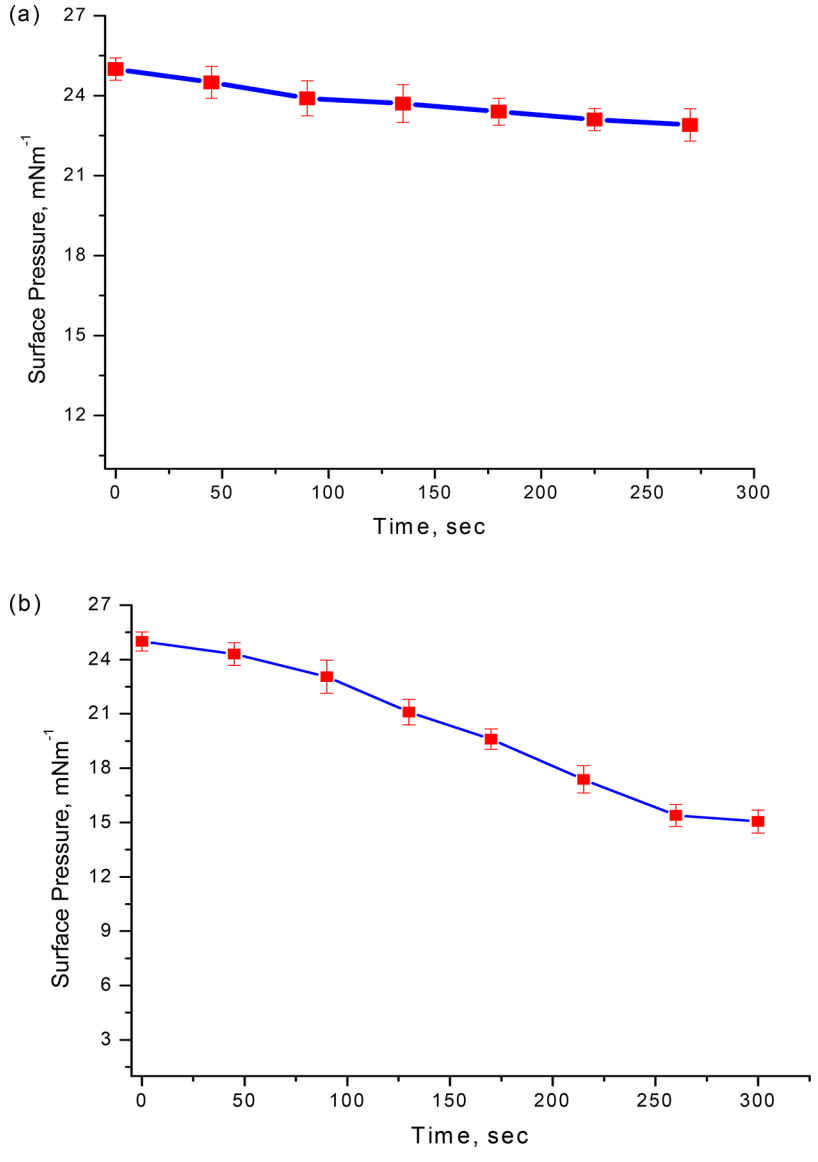

Figure 9. Surface pressure vs time shows the drop of surface pressure in absence (a) and presence (b) of green LED light. Magnitudes of error bars are calculated as the standard deviation from three experiments.

higher surface pressures, the intensity of the absorbance increased proportionally. While plotting the surface pressure vs absorbance at 233 and 278 nm, we found that absorbance increases proportionally with the surface pressure within the

DOI: 10.1021/acs.langmuir.8b03505
Langmuir 2019, 35, 2814−2820

experimental error as shown in Figure 6. The slopes of the curves were also almost equal to each other. This observation confirms that the formation of a homogeneous FB1 Langmuir monolayer at the air−water interface occurs before the monolayer attains the collapse surface pressure. Moreover, it also gives an idea of the stability of the monolayer. If the monolayer was unstable, the absorbance would not increase steadily but would rather reach a plateau as the molecules are forced to submerge into the water subphase.[29]

3.1.4. In Situ Fluorescence Spectroscopy of the Langmuir Monolayer. From in situ UV−vis spectroscopy, the homogeneity and the stability of the FB1 Langmuir monolayer were also observed. To confirm this finding, we performed in-situ fluorescence spectroscopy of the monolayer as shown in Figure 7 a. Further, we obtained a linear relationship (Figure 7 b) by plotting intensity versus surface pressure at 307 nm. This investigation ruled out the hypothesis of loss of analyte in the water during the formation of the Langmuir monolayer.

3.1.5. Effect of LED Light Irradiation on the FB1 Langmuir Monolayer. To study the impact of green light on the Langmuir monolayer of FB1 molecules, an experimental setup was built as shown in Figure 8. For this study, the monolayer was compressed to 25 $mN{\cdot}m^{-1}$ and was kept still without further compression. The green LED light (525 nm) placed approximately 2 mm above the monolayer irradiated the Langmuir monolayer continuously for 5 min, and the decrease in surface pressure was recorded with respect to time. Figure 9 shows the difference in the decrease of surface pressure in the absence and presence of green light. It was found that almost a 37% decrease in surface pressure was observed in the comparisons between the absence and presence of green LED light. This decrease in surface pressure clearly demonstrates that the toxin is propelled strongly into the water subphase during irradiation with green LED light. The sinking of the toxin into the subphase can be due to the formation of photoproducts related to the degradation of the toxin.

4. COMPARATIVE STUDY OF THE EFFECT OF 525 NM LED LIGHT ON FB1 IN AQ METHANOL SOLUTION

After the observation of the degradation of the FB1 Langmuir monolayer under green LED light irradiation, it was important to compare this result to that of FB1 in solution. For this, we carried out the experiment in which fluorescence spectrum was recorded. In this method, FB1 was irradiated with green light for 20 s in intervals of 5 min for a total of 70 min. Figure S1 shows the photoluminescence spectra of FB1 before and after treatment with green LED light. We can clearly see that there is a significant decrease in the photoluminescence of FB1 after irradiation with green light. We also observed a shift of the maximum peak from 370 to 359 nm. The intensity maxima decreased by 38% after 70 min. In the meantime, we also saw that there was evolvement of another new peak centered at 343 nm. This clearly showed that the green LED light had degraded the FB1 molecule.

To further confirm the degradation of FB1 due to the irradiation, we conducted a UV−vis experiment. Figure S2 shows the absorbance spectra of FB1 before and after the treatment with light. The FB1 molecule usually in a normal state has an absorption at 278 nm,[30] but after passing light, the absorption bands changed. This data clearly shows the change in absorbance maxima which further fortifies the hypothesis that green LED light degrades the FB1 molecule. Here, it is to be noted that FB1 was dissolved in aqueous methanol (CH_3OH/H_2O = 1:5), so the solvent effect has been pronounced in the spectra.

Figure S3 shows the mass spectrum in the absence and presence of the irradiated sample. We can clearly see a molecular ion peak at 722.39 (+1) m/z peak which is due to the FB1 molecule whose molecular mass is 721.83 m/z. After treatment with light, we saw a change in the spectrum with the evolvement of other peaks. This shows that the native structure of FB1 changes to some extent due to the application of green LED light. On the C-14 and C-15 atoms of the FB1 molecule, terminal carboxyl groups of propane-1,2,3-tricarboxylic acid or tricarballylic acid (TCA) are attached. These TCA moieties are very susceptible to fragmentation by the FB1 molecule due to irradiation with LED. The molecular ion peak at 528.0215 m/z is due to the loss of one TCA and one O−H group. The molecular ion peak at 301.3463 (+1) m/z is due to the hydrocarbon backbone of FB1 when the TCA moieties H_2O and $-NH_2$ are lost due to irradiation with LED light.

5. CONCLUSION

The self-assembly ability of the analytes to organize spontaneously mimicking living cell membranes, appears to be a suitable concept for the development of biomimetic membrane models. The Langmuir monolayer of analyte like FB1 provides the potential of two-dimensional molecular self-assemblies, which have been extensively used as models to understand the role and the organization of biological membranes and their interactions. The observed interfacial property showed that FB1 remains potently active on the Langmuir monolayer. Upon treatment with green LED light, we found that the FB1 Langmuir monolayer gets degraded. This clearly indicates that the tendency of FB1 molecules to stay active on the cell membrane will decline and their penetrating ability on the membrane will get diminished. Ultimately, the toxin will not get a chance to reach the cell and the associated infection of the cell can be avoided.

■ ASSOCIATED CONTENT

Supporting Information

The Supporting Information is available free of charge on the ACS Publications website at DOI: 10.1021/acs.langmuir.8b03505.

Emission spectra, UV−vis spectra, and the mass spectra of the fumonisin B1 (FB1) aq methanol solution having concentration of 2.8×10^{-4} M before and after being treated with green LED light (PDF)

■ AUTHOR INFORMATION

Corresponding Author

*E-mail: rml@miami.edu. Phone +1-305-284-2194. Fax: +1305-284-6367.

ORCID

Roger M. Leblanc: 0000-0001-8836-8042

Notes

The authors declare no competing financial interest.

■ ACKNOWLEDGMENTS

This work was supported by NIH grant # GR-009887; NSF grant # GR-011298 (Dr. Leblanc's Lab); Florida Lions Eye Bank; Beauty of Sight Foundation; Drs. K. R. Olsen, M. E.

DOI: 10.1021/acs.langmuir.8b03505
Langmuir 2019, 35, 2814−2820

Hildebrandt, Raksha Urs, and Aaron Furtado; University of Miami Scientific Awards Committee Interdisciplinary Team Science Pilot Award (UM SAC 2016-17); The D. and Janet K. Robson Foundation; and The Ophthalmic Biophysics Center core funds (Dr. Parel Lab). We thank Cornelis J. Rowaan BSEME for building the LED power supply to our specifications. S.K.S. is also thankful to Mr. Qiaoyu Hu for helping in computer simulation work.

REFERENCES

(1) Naiker, S.; Odhav, B. Mycotic keratitis: profile of Fusarium species and their mycotoxins. *Mycoses* **2004**, *47*, 50−56.
(2) Shetty, P. H. *Natural occurrence and management of Fumonisin mycotoxins*; Lambert Academic Publishing: 2011.
(3) Thomas, P.; Kaliamurthy, J. Mycotic keratitis: epidemiology, diagnosis and management. *Clin. Microbiol. Infect.* **2013**, *19*, 210−220.
(4) Desjardins, A.; Proctor, R. Molecular biology of Fusarium mycotoxins. *Int. J. Food Microbiol.* **2007**, *119*, 47−50.
(5) Marasas, W. F. O.; Nelson, P. E.; Toussoun, T. A. *Toxigenic Fusarium species. identity and mycotoxicology*; Pennsylvania State University: 1984.
(6) Seo, J.-A.; Proctor, R. H.; Plattner, R. D. Characterization of four clustered and coregulated genes associated with fumonisin biosynthesis in Fusarium verticillioides. *Fungal Genet. Biol.* **2001**, *34*, 155−165.
(7) Rheeder, J. P.; Marasas, W. F.; Vismer, H. F. Production of fumonisin analogs by Fusarium species. *Appl. Environ. Microbiol.* **2002**, *68*, 2101−2105.
(8) Blackwell, B.; Edwards, O.; Fruchier, A.; ApSimon, J.; Miller, J. NMR structural studies of fumonisin B 1 and related compounds from Fusarium moniliforme. In*Fumonisins in Food*; Springer: 1996, 75−91.
(9) Plattner, R. D.; Weisleder, D.; Poling, S. M., Analytical determination of fumonisins and other metabolites produced by Fusarium moniliforme and related species on corn. *Fumonisins in Food*; Springer: 1996, 57−64.
(10) Momany, F. A.; Dombrink-Kurtzman, M. A. Molecular dynamics simulations on the mycotoxin fumonisin B1. *J. Agric. Food Chem.* **2001**, *49*, 1056−1061.
(11) Xie, L.; Dong, X.; Shi, W. Treatment of fungal keratitis by penetrating keratoplasty. *Br. J. Ophthalmol.* **2001**, *85*, 1070−1074.
(12) Galperin, G.; Berra, M.; Tau, J.; Boscaro, G.; Zarate, J.; Berra, A. Treatment of fungal keratitis from Fusarium infection by corneal cross-linking. *Cornea* **2012**, *31*, 176−180.
(13) Bunya, V. Y.; Hammersmith, K. M.; Rapuano, C. J.; Ayres, B. D.; Cohen, E. J. Topical and oral voriconazole in the treatment of fungal keratitis. *Am. J. Ophthalmol.* **2007**, *143*, 151−153.
(14) Yoon, K.-C.; Jeong, I.-Y.; Im, S.-K.; Chae, H.-J.; Yang, S.-Y. Therapeutic effect of intracameral amphotericin B injection in the treatment of fungal keratitis. *Cornea* **2007**, *26*, 814−818.
(15) Chang, H.-Y. P.; Chodosh, J. Diagnostic and therapeutic considerations in fungal keratitis. *Int. Ophthalmol. Clin.* **2011**, *51*, 33−42.
(16) Shih, M.-H.; Huang, F.-C. Effects of photodynamic therapy on rapidly growing nontuberculous mycobacteria keratitis. *Invest. Ophthalmol. Visual Sci.* **2011**, *52*, 223−229.
(17) Kharkwal, G. B.; Sharma, S. K.; Huang, Y. Y.; Dai, T.; Hamblin, M. R. Photodynamic therapy for infections: clinical applications. *Lasers Surg. Med.* **2011**, *43*, 755−767.
(18) Arboleda, A.; Miller, D.; Cabot, F.; Taneja, M.; Aguilar, M. C.; Alawa, K.; Amescua, G.; Yoo, S. H.; Parel, J.-M. Assessment of rose bengal versus riboflavin photodynamic therapy for inhibition of fungal keratitis isolates. *Am. J. Ophthalmol.* **2014**, *158*, 64−70.
(19) Amescua, G.; Arboleda, A.; Nikpoor, N.; Durkee, H.; Relhan, N.; Aguilar, M. C.; Flynn, H. W.; Miller, D.; Parel, J.-M. Rose Bengal photodynamic antimicrobial therapy: A novel treatment for resistant Fusarium keratitis. *Cornea* **2017**, *36*, 1141−1144.
(20) Höfs, S.; Mogavero, S.; Hube, B. Interaction of Candida albicans with host cells: virulence factors, host defense, escape strategies, and the microbiota. *J. Microbiol.* **2016**, *54*, 149−169.
(21) Hostetter, M. K. Adhesins and ligands involved in the interaction of Candida spp. with epithelial and endothelial surfaces. *Clin. Microbiol. Rev.* **1994**, *7*, 29−42.
(22) Sharma, S. K.; Li, S.; Micic, M.; Orbulescu, J.; Weissbart, D.; Nakahara, H.; Shibata, O.; Leblanc, R. M. *β*-Galactosidase Langmuir monolayer at air/X-gal subphase interface. *J. Phys. Chem. B* **2016**, *120*, 12279−12286.
(23) Bonanno, J. A.; Polse, K. Measurement of in vivo human corneal stromal pH: open and closed eyes. *Invest. Ophthalmol. Vis. Sci.* **1987**, *28* (3), 522−530.
(24) Krieger, E. YASARA: 2003.
(25) Šegvić, M.; Pepeljnjak, S. Fumonisins and their effects on animal health-a brief review. *Vet. Arhiv.* **2001**, *71* (5), 299−323.
(26) Sharma, S. K.; Seven, E. S.; Micic, M.; Li, S.; Leblanc, R. M. Surface chemistry and spectroscopic study of a Cholera toxin B Langmuir monolayer. *Langmuir* **2018**, *34*, 2557−2564.
(27) Thakur, G.; Wang, C.; Leblanc, R. M. Surface chemistry and in situ spectroscopy of a lysozyme Langmuir monolayer. *Langmuir* **2008**, *24*, 4888−4893.
(28) Sobczyk, L.; Grabowski, S. J.; Krygowski, T. M. Interrelation between H-bond and Pi-electron delocalization. *Chem. Rev.* **2005**, *105*, 3513−3560.
(29) Crawford, N. F.; Micic, M.; Orbulescu, J.; Weissbart, D.; Leblanc, R. M. Surface chemistry and spectroscopy of the *β*-galactosidase Langmuir monolayer. *J. Colloid Interface Sci.* **2015**, *453*, 202−208.
(30) Wang, Y.; He, C.-H.; Zheng, H.; Zhang, H.-B. Characterization and comparison of fumonisin B1-protein conjugates by six methods. *Int. J. Mol. Sci.* **2012**, *13*, 84−96.

DOI: 10.1021/acs.langmuir.8b03505
Langmuir 2019, 35, 2814−2820